学 位 論 文 の 要 旨

論文題目　Bifurcation of Oscillatory Motion in Self-Propelled Objects at an Air/Water Interface
(水面滑走する自己駆動体における振動運動の分岐現象)

広島大学大学院統合生命科学研究科
数理生命科学プログラム
学生番号　D196399
氏　　名　XU　YU

Self-propelled objects are used to describe that the objects can autonomously move by converting energy from the environment. Various types of self-propelled objects have been studied to understand the mechanism of characteristic motion and to create artificial motors that respond to the change in the external environments [1, 2]. However, the autonomy of non-living systems is low, since the self-propelled objects in non-living systems exhibit generally unidirectional or random motion. The biological systems (e.g., bacterial, walking, or swimming animals) have inspired the design and enhancement of the autonomy of these objects. Because the nonlinear phenomena (e.g., oscillation, synchronization, and bifurcation) are frequently observed in biological systems, this suggests that the autonomy of non-living systems is lower than that of biological systems. Several studies have indicated that the autonomy of the self-propelled objects can be enhanced by coupling a nonlinear phenomenon with a self-propelled motion [1, 2]. In this research, I designed three types of self-propelled objects by introducing the nonlinear phenomena to study the characteristic features of the motion and explain the mechanism of the characteristic motion.

A camphor disk on the water surface is one of the simple and available self-propelled objects since it is easy to manufacture and exhibits motion keeping long time. The driving force of motion is the difference in the surface tension generated by the camphor molecules around the object. Therefore, the dissolution and diffusion of camphor molecules around the object play an important role in the nature of motion. For example, the surfactant dissolved in a water phase as a suppressing force can induce the characteristic self-propelled motion by controlling the dissolution of camphor molecules from the camphor disk. In this section [3], the oscillatory phenomenon was introduced into the self-propelled motion by the addition of the surfactant. I designed a self-propelled camphor object consisting of a camphor disk and a plastic sheet (Figure 1) to study the influence of the contact area on the self-propulsion. Here, the contact area between the bottom of the disk and sodium dodecyl sulfate (SDS) aqueous phase (S in mm^2) as a variable parameter was changed using a circular plastic sheet with different diameters. SDS dissolved in a water phase (10 mM) as a surfactant was used to create an oscillatory motion by

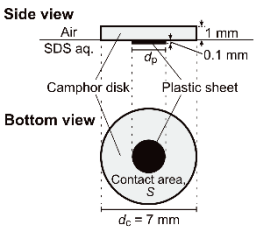

Figure 1 . Schematic diagram of the camphor object.

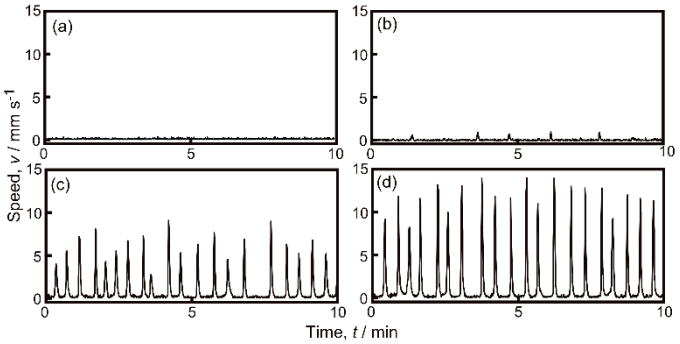

Figure 2. Time variation of the speed of a camphor object at different S = (a) 10.2, (b)18.9, (c) 25.9, and (d) 38.5 mm^2.

reducing the surface tension of water. The camphor object shows the oscillatory motion (alternation between the resting and moving states) and no motion depending on the varying contact area (Figure 2). Motion features, that is, the maximum speed, frequency of oscillatory motion, and mode bifurcation, varied depending on *S*. With an increase in *S*, the period of oscillatory motion is maintained and the maximum speed is increased. I discussed the mode bifurcation and motion features based on the number of camphor molecules accumulated at the base of the object and the formation of the SDS–camphor complex. In the case of no motion at a smaller *S*, the SDS molecular layer adsorbed on the surface of the aqueous phase inhibits the development of the complexes and camphor molecules to the surface of the aqueous phase. In the case of a larger *S*, a large number of the SDS–camphor complex around the object as a driving force can accelerate the camphor object. The results suggest that the nature of the oscillatory motion can be controlled by the contact area between the self-propelled and the external enverinment.

In this section [4], the speed of the self-propelled camphor disk placed on the sodium dodecyl sulfate (SDS) aqueous phase depending on the depth of the aqueous phase (*d*) was described. The speed of the self-propelled motion for the deeper aqueous phase was higher than that for the shallower aqueous phase at the concentration of SDS (C_{SDS}) lower than 0.1 mM. However, a reverse dependence of speed on the water depth was observed at the C_{SDS} higher than 0.3 mM (Figure 3). A bifurcation of C_{SDS} for the dependence of speed on depth was observed at 0.2 mM. The change in surface tension of SDS solution after the addition of the camphor disk, and effective diffusion of the camphor on the aqueous surface at different depths were measured to verify the inversion mechanism of the dependence. In addition, the opposite dependency is qualitatively reproduced by numerical calculation based on the Navier-Stokes equation, the reaction-diffusion-advection equation, and the surface tension of camphor. Based on the results of experimental and numerical calculation, the opposite dependency is explained as follows, at the lower C_{SDS}, a deeper aqueous phase induces a stronger Marangoni flow and a greater effective diffusion coefficient (*D*) since the lower friction at the bottom wall. In contrast, at the higher C_{SDS}, the number of camphor molecules is lower in the deeper aqueous phase since the formation of the SDS–camphor complex. This induces strong Marangoni flow and a greater *D* for the shallower aqueous phase. Combined, the opposite dependence of speed on the depth was determined by the competition between the consumption rate of SDS in the aqueous phase and the friction of the bottom wall.

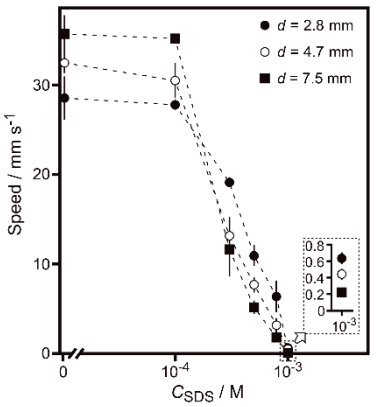

Figure 3. Average speed of the self-propelled motion of a camphor disk versus C_{SDS} depending on the concentration of SDS at different depths of the aqueous phase, *d*.

Introducing chemical reactions to self-propelled objects is one of the strategies to promote the autonomy and diversity of self-propelled objects in non-living systems. In this section [5], a urease motor consisting of a plastic object and a filter paper with urease was constructed (Figure 4). I introduced a reaction of urea ($(NH_2)_2CO + 3H_2O \xrightarrow{urease} HCO_3^- + 2NH_4^+ + OH^-$) into a self-propelled object to achieve the mode change of motion for the urease motor by controlling the initial pH (pH_{ini}) of an aqueous solution. The driving force of self-motion for the urease motor was the difference in surface tension induced by the ammonia produced by the enzyme reaction. The oscillatory motion of the urease motor was observed at pH_{ini} = 5.0 and 5.5. In contrast, at lower and higher pH_{ini}, the urease motor exhibits no motion (Figure 5). A bifurcation between oscillatory motion and no motion was

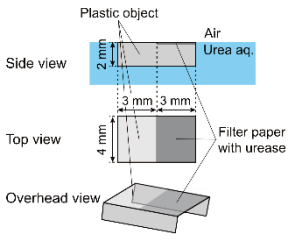

Figure 4 . Schematic diagram of the urease motor.

observed at pH_{ini} = 4.0 and 6.5. The existence of the no motion at a certain pH_{ini} suggests that the rates of enzyme reaction at pH < 4.0, and pH > 6.5, are lower than those at 4.0 ≤ pH ≤ 6.5, since lower and higher pH_{ini} reduce the activity of urease, making it difficult for the urease motor to produce ammonia as the source for the driving force of motion. Within the range of oscillatory motion, both the frequency and maximum speed increased at 4.0 ≤ pH_{ini} ≤ 5.5 but decreased at 5.5 ≤ pH_{ini} ≤ 6.5 with an increase in pH_{ini}. The synchronization between pH oscillation and the speed of oscillatory motion was also observed. The results indicate that the frequency and maximum speed of oscillatory motion are determined by pH-sensitive enzyme activity for urease. The mechanism and nature of the oscillatory motion are discussed based on the bell-shaped activity-pH curve of urease and the surface tension around the urease motor. The mechanism of the oscillatory motion at pH_{ini} = 5.0 was schematically shown in Figure 6. At State I, the urease motor remains the resting state since the rate of the enzyme reaction is low at the lower pH_{ini}. As the pH increases by the production of ammonia around the tail of the motor, the autocatalytic production of ammonia was induced by the increase in pH since the increase in the enzyme activity. When the concentration of ammonia reaches the threshold value, the urease motor can be accelerated by the difference in the surface tension around the urease motor at State II. At State III, the urease motor returns to the resting state because the motor moves to a point on the aqueous surface with a lower pH. Thus, oscillatory motion is repeated between resting and moving states.

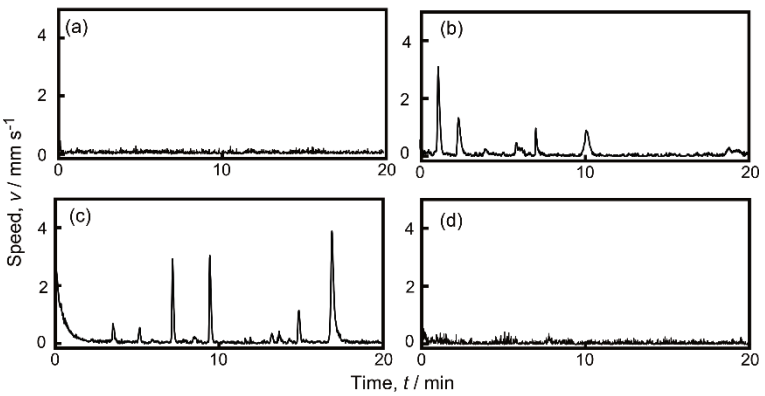

Figure 5. Time variation of the speed of a urease motor at different initial pH, pH_{ini} = (a) 3.5, (b) 5.0, (c) 5.5, and (d) 7.0.

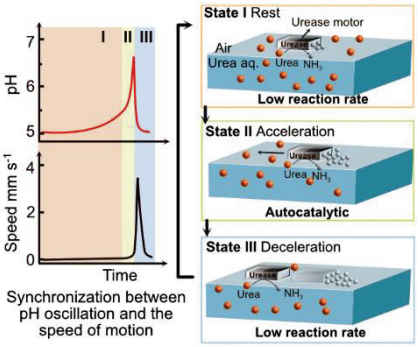

Figure 6 . Mechanism of the oscillatoty motion

In summary, I designed three self-propelled objects that show the characteristic nonlinear phenomena, which can respond to the internal and external environments. In this research, I achieved the enhancement of the autonomy in self-propelled objects and the molecular control of the characteristic features of motion. The mathematical model was constructed to reproduce the experimental results. In addition, coupling chemical reactions to self-propelled objects is one of the breakthrough ideas to promote the autonomy of self-propelled objects. This study provides several strategies for designing self-propelled objects and explanations regarding the motion mechanism. It is significant from both fundamental and practical perspectives to understand how self-propelled objects exhibit regular motion and to establish ways of controlling their motion.

References

[1] N. J. Suematsu, S. Nakata. *Chem. Eur. J.* 2018, 24, 6308−6324.
[2] S. Nakata, V. Pimienta, I. Lagzi, H. Kitahata, N. J. Suematsu. *RSC-ebook* 2018, ISBN: 789-1-78801-166-2.
[3] Y. Xu, N. Takayama, H. Er, S. Nakata. *J. Phys. Chem. B* 2021, 125, 1674–1679.
[4] Y. Xu, N. Takayama, Y. Komasu, N. Takahara, H. Kitahata, M. Iima, S. Nakata. *Colloids Surf. A Physicochem. Eng. Asp.* 2022, 635, 128087.
[5] Y. Xu, L. Ji, S. Izumi, S. Nakata. *Chem. Asian J.* 2021, 16, 1762– 1766.